

REVIEWER #1:

General comments:

In this paper, the authors analyze the spatial distribution of decorrelation ranges on the east coast of Australia using the semivariogram approach. The decorrelation scale analysis at east coast of Australia is relatively new. Over all, the quality of the work done and of the manuscript are adequate. However, more details are needed in order to make the content clearer and more understandable. Below are some comments that I hope can be used to improve the manuscript.

We thank the reviewer for his/her positive comments. We have now enhanced the clarity of the manuscript and provided more details about the method and results. Please find the details below.

Specific comments:

1. More details of the equations are needed in order to let readers understand the method the authors use. For example: 1) Equation (1): what does “variance” represent in this equation? Variance of what? Please specify. 2) Equation (2): what the general physical meaning of this equation? Why is equation (2) more robust than equation (1)? What do the number 0.457 and 0.494 represent? Why the 4th square in this equation? The details of this equation is especially important because this is the whole paper based on. 3) Equation (3): The author explain the meaning of sill, nugget and the range in this equation, but what is the meaning of this equation in general? Why do the authors separate it into 3 sections ($h=0$, $0 < h < r$)? What are the 3/2 and 3rd square mean? What is the benefits and drawback of this equation?

Equation 1:

Variance of $[Z(x)-Z(x+h)]$ is changed into $\frac{1}{2} \frac{1}{N} \sum (Z(x) - Z(x+h))^2$ for more clarity.

Equation 2:

We thank the reviewer for pointing out the need for more details to explain equation 2, which are now included in the manuscript.

“In this equation, the power $\frac{1}{2}$ comes from a fourth-root of $[Z(x)-Z(x+h)]^2$ that reduces the skewness in the distribution, thereby approaching a Gaussian process. The 4th square acts to correct the scale and returns the same units as equation 1, while the denominator adjusts the bias resulting from the whole transformation. This estimate is more robust statistically in the sense that the mean can be applied to the new distribution. Compared to equation 1, the semivariogram is only slightly modified for the highest lags when using equation 2, but the parameters (sill, range and nugget that are investigated in section 3 remain very similar.”

Equation 3 is the definition of a classic spherical (or Matheron) model as opposed to other mathematical models such as a linear plateau, Gaussian or exponential models. They can all be fitted to semivariograms in order to extract the parameters of interest (see Biswas and Si, 2013, for a complete description of the different models). Two additional models were tested but were less adequate in terms of sum of squared error (sse) and adjusted R-square statistics for the fit (see last paragraph in section 2.2).

2. Figure 3 lower left panel. Compared with across-shelf Temperature, Salinity, Fluorescence and DO, the across-shelf distance of CDOM extends more than 20 km, while all other variables are limited to less than 20 km (left panel a, b, c, and d). Why is that? I didn't find the explanation in the manuscript. Please explain.

We thank the reviewer for pointing this out. Cross-shelf semivariogram for CDOM was performed for distance lags for which there were more than 5 glider missions as opposed to other variables (10 glider missions) for which the good fit allowed to be more selective and add significance to the statistics. Again, this is because statistics on CDOM appeared to be more challenging than other variables due to the poor quality dataset. The minimum of 30 valid data pairs per lag that was defined by Journel and Huijbregts (1978) is however kept, as in Doney et al. (2003). This is now specified in the manuscript. The extended data (lower threshold on the number of glider missions) required to successfully fit the mathematical model to the across-shelf CDOM semivariogram explains the extended x-axis (to lags up to 25 km) in Fig. 3 lower left panel.

REFERENCE:

Journel, A. G., Huijbregts, C.J., 1978. Mining Geostatistics, Academic Press Inc, London, UK

3. In figure 2, the authors separate the analysis into 12 months. Why not do the same for figure 3? Please explain.

While SST observations are provided every day with a good spatial coverage (except for cloud cover), glider missions are sparse and not numerous enough to break them down into months. As specified in the discussion, we expect that spatial scales may vary seasonally, particularly in the biological parameters. This will be tested when we have sufficient data in each season. We still believe that the monthly information supplied in Fig. 2 on top of the annual mean provides valuable information on how seasons may affect the variance, but barely the range of the SST.

4. Due to the method used here is highly empirical, the authors should discuss the advantages and limitations of the method.

A paragraph discussing the advantages and limitations of the method is now included in the discussion.

“As for all statistics, limitations arise from the amount of data used (especially along the shelf where the data density is smaller) and contamination of the dataset (for instance CDOM). In geostatistics, uneven spatial distribution of the observations over the analyzed area can be a limitation as well but remains difficult to quantify. The major advantage of the semivariogram method used is that it can be applied to sparse dataset like glider observations, as opposed to spatial autocorrelations for instance. It allows to objectively compare interesting parameters (range, sill, nugget) for different variables, directions and depths. In this study, the results compare well when using different statistical fits, and are consistent with expected outcomes based on previous knowledge of local dynamics and related studies in other regions.”

5. Decorrelation scale is the analysis variable of this manuscript, and it is also one of the most important parameters in setting up data assimilation procedures. The authors mentioned the observational errors and representation errors in the data assimilation section, but they didn't

mention decorrelation scale at all, which should be the center of this paper. I suggest the authors to add discussion of decorrelation scale in this section. The following paper is an example setting up data assimilation projection space according to decorrelation scales: Pan, C., Yaremchuk, M., Nechaev, D., 2011. Variational assimilation of glider data in the Monterey Bay. *Journal of Marine Research* 69 (2-3), 331-346.

We thank the reviewer for the relevant reference. A paragraph has been added in the discussion (section 4.4).

“There are a variety of data assimilation systems based upon two broad approaches, ensemble methods (e.g. Oke et al. 2008, Jones et al., 2012) and variational methods, that minimize a cost function (e.g. Moore et al., 2011). Regardless of the approach used, assumptions are made about the spatial footprint of an observation, for which a key parameter is the decorrelation length scale. Within the ensemble (e.g. Oke 2008) and hybrid (Pan et al., 2011) data assimilation approaches, covariance localization (Sakov and Bertino 2011) is used to increase the rank of the background error covariance matrix. The anisotropic (along-shelf and cross-shelf) ranges presented in this study and method used to derive them, allows for the direct calibration of the decorrelation scales enforced within most data assimilation systems that are currently in use. Additionally, estimates of how these decorrelation scales vary in time is also available (e.g. Figure 2), suggesting that an optimally tuned data assimilation system should allow for temporal variation in the localization or provide an assessment of the temporal variability of the ensemble from an Ensemble Kalman Filter (EnKF) system.”

REFERENCES:

*Jones, E.M., Oke, P.R., Rizwi, F. and Murray, L.M., 2012. Assimilation of glider and mooring data into a coastal ocean model. *Ocean Modelling*, 47, pp.1-13.*

*Moore, A.M., Arango, H.G., Broquet, G., Powell, B.S., Weaver, A.T. and Zavala-Garay, J., 2011. The Regional Ocean Modeling System (ROMS) 4-dimensional variational data assimilation systems: Part I—System overview and formulation. *Progress in Oceanography*, 91(1), pp.34-49.*

*Oke, P.R., Brassington, G.B., Griffin, D.A. and Schiller, A., 2008. The Bluelink ocean data assimilation system (BODAS). *Ocean Modelling*, 21(1), pp.46-70.*

*Pan, C., Yaremchuk, M., Nechaev, D. and Ngodock, H., 2011. Variational assimilation of glider data in Monterey Bay. *Journal of Marine Research*, 69(2-3), pp.331-346.*

*Sakov, P. and Bertino, L., 2011. Relation between two common localisation methods for the EnKF. *Computational Geosciences*, 15(2), pp.225-237.*

6. According to figure 1, all glider observations are confined within 200 m isobath. This means the decorrelation scales are all confined within 200 m isobaths. So how does this affect cross-shelf decorrelation scales?

As specified in the title, we only consider shelf dynamics and define the outer end of the continental shelf as the 200 m isobath, consistent with previous studies. The geometry of the shelf (‘relatively narrow, between 16 and 70 km (mean of 37 km)’) definitely influences the cross-shelf decorrelation scales, as specified in the manuscript. Still, the variability of cross-shelf scales found between different depths and different parameters and the isotropic patterns give new insights into the regional dynamics that are not only related to the geography of the area.

Minor comment:

Figure 1: “Across-shelf” does not seem to be a normal word. “cross-shelf” might be more appropriate.

This has been modified throughout the manuscript.

According to my observation, I believe this paper is well-organized. The method the author used is straightforward, and the figures support the results, although more details are needed to enrich the content. Therefore, I recommend minor revision.

We believe that the new version of the manuscript is now more detailed and improved, and thank the reviewer for his/her contribution.

REVIEWER #2:

This manuscript uses an extensive set of observations on the southeast Australian continental shelf to estimate the scales of variability of various factors. As discussed in the manuscript, knowledge of such scales is critical to designing observational and modeling systems that resolve key processes. I find no major faults in the manuscript, but have a number of questions and comments that the authors should address to improve the manuscript.

We thank the reviewer for his/her interest and relevant questions that helped us improving the manuscript.

1. The description of gliders and the sampling (page 20104) is a bit too vague, and at times somewhat inaccurate. A citation to a general glider reference (e.g., Davis et al. 2003 or Rudnick, et al. 2004) would be helpful for the reader. The statement that gliders 'use seawater to change their buoyancy' is not particularly accurate; each type of glider changes its volume (by either moving oil between internal and external bladders or displacing seawater), thereby changing its buoyancy to rise and fall. This vertical motion is translated into forward motion by wings and controlling the glider's pitch, resulting in a sawtooth path through the water. [I'm sure the authors know this, but they should include it for the sake of unfamiliar readers.] Stating that the 'average horizontal displacement between two dives is around 200 m' is probably true, but somewhat misleading; shallower dives have closer horizontal (and temporal spacing) and so there are more of them, biasing the 'average horizontal displacement' small. Dives to 100 m should be separated by ~500 m in calm water; dives to 200 m by ~1000 m; and so on. Over the deeper part of the shelf, resolution is much less than the 200 m average reported, so I suggest the authors clarify this point.

The glider description has been improved and detailed: "Ocean gliders are autonomous underwater vehicles which change their buoyancy to dive up through the water column. Without propulsion, this vertical motion is transformed into horizontal momentum using the vehicle's wings, while its pitch controls the forward motion. During the resulting vertical sawtooth pattern through the water column, a wealth of scientific observations are recorded and analyzed here."

The reviewer is right, the distance travelled over ground between dives directly depends on the dive depth, which is now clarified in the manuscript: "The horizontal displacement between two dives increases with the depth of the dive, with median over ground distances from 130m (for dives in 25 - 50m of water) to 1100m (in 150 - 200m of water)."

2. Are salinity measurements from pumped or unpumped CTDs? If unpumped, how significant is salinity spiking in areas of large temperature gradients? How does this affect the scale analysis?

As the large dataset includes deployments from 2008, some of the vehicles were equipped with an unpumped CTD. However, a salinity spike correction is routinely performed in the quality control procedure. We therefore do not expect this common issue to affect the scale analysis presented. It is now specified: "including a salinity spike correction due to the use of unpumped CTDs in early deployments."

3. The definition of the structure function (Eq. 1) could be more clearly presented as $1/2$ the mean

square difference between values at a given separation. The empirical formulation for the structure function (Eq. 2) needs more description, particularly the empirical constants.

More explicit descriptions on equation 2 was also requested by Referee 1. We thank the reviewer for the useful suggestion.

For equation 1, variance of $[Z(x)-Z(x+h)]$ has been changed into $\frac{1}{2} \frac{1}{N} \sum (Z(x) - Z(x+h))^2$ and described as “half the mean square difference between values at a given separation h ” following the reviewers’ suggestion.

Equation 2 is now further described in the manuscript:

“In this equation, the power $\frac{1}{2}$ comes from a fourth-root of $[Z(x)-Z(x+h)]^2$ that reduces the skewness in the distribution, thereby approaching a Gaussian process. The 4th square acts to correct the scale and returns the same units as equation 1, while the denominator adjusts the bias resulting from the whole transformation. This estimate is more robust statistically in the sense that the mean can be applied to the new distribution. Compared to equation 1, the semivariogram is only slightly modified for the highest lags when using equation 2, but the parameters (sill, range and nugget that are investigated in section 3 remain very similar.”

4. Page 20105, lines 4-5: Why pairs within 0.1 degrees? Perhaps give the distance in kilometers for clarity.

In order to investigate anisotropy, data have to be constrained in the opposed direction (meridional / along-shelf when analyzing zonal / cross-shelf semivariogram and inversely). We chose 0.1 degrees, as it still allows a sufficient number of measurement pairs (a minimum of 30 valid data pairs per lag was suggested by Journel and Huijbregts, 1978). The manuscript now specifies “0.1° (~10 km)”.

REFERENCE:

Journel, A. G., Huijbregts, C.J., 1978. Mining Geostatistics, Academic Press Inc, London, UK

5. Regarding homogeneity of the statistics: Lumping observations together to calculate structure functions assumes homogeneity in the statistics. I would expect that there is a change in scales from the inner to outer shelf that could perhaps be diagnosed from these observations. Lack of homogeneity in the vertical is more concerning; surely statistics in the mixed layer differ (vertical scale ~ mixed layer depth?) from those in the thermocline (small vertical scale?) and from those below the thermocline (longer vertical scale?).

Homogeneity in the statistics can indeed be issue, in particular in the water column which is characterized by multiple spatial scales. Semivariograms do not identify multiple scales but only the dominant scales, which is why we do not expect to resolve the smallest vertical scales through the thermocline. Considering the good vertical resolution of the dataset, this could probably be addressed using autocorrelation functions, but will require further investigation.

6. There is a good bit of flipping back and forth between ‘semivariogram’ and ‘structure function’; best to pick one and stick with it.

This has been modified throughout the manuscript, keeping the term “semivariogram”.

7. I find the terms 'sill', 'range', and 'nugget' difficult to follow, though the authors make a good effort to clarify them. 'Range' is particularly troublesome in usages like (page 20108, Line 25) 'mean temperature ranges...' since range typical means the difference between minimum and maximum value of a variable. Consider not using these particular terms.

Unfortunately “sill”, “range”, and “nugget” are the standard terms used when describing semivariograms. We have clarified the term ‘range’ throughout the manuscript, by replacing it by “decorrelation range”, “semivariogram range” or “length scale”.

8. Page 20113, lines 12-13: this is not a complete sentence.

We thank the reviewer for pointing out this mistake. It now reads: “The length scales calculated here can be used to guide the design of ocean observing systems, in particular to answer questions related to the observation density needed to resolve along and across shore variability in both the physical and biological parameters.”

REVIEWER #3:

The reference to Schaeffer et al. (2015; cited on p. 20105), which refers to details on the data processing, is missing from the list of references. If it has not been published yet, then it would be helpful to include these details in the present paper.

There are two references providing details on the data processing, especially the way the glider profiles from all deployments were gridded and averaged to provide a mean state of the ocean variables (used here to compute the anomalies $Z(x)$). The first one is Schaeffer et al, 2015, available in Geophysical Research Letters:

Schaeffer, A., and M. Roughan, 2015: Influence of a western boundary current on shelf dynamics and upwelling from repeat glider deployments. Geophysical Research Letters, 42, 121 - 128, doi:10.1002/2014GL062260.

Unfortunately the second one, Schaeffer et al., 2016, which is a data descriptor and provides more information on biogeochemical data and individual glider deployments, is still in review at this time:

Schaeffer, A., M. Roughan, T. Austin, B. Hollings, E. King, A. Mantovanelli, S. Milburn, B. Pasquer, C. Pattiaratchi, R. Robertson, I. Suthers, D. White: Mean hydrography on the continental shelf from 25 repeat glider deployments along Southeastern Australia. Scientific Data, in review.

We are hoping that it would be available before the final version of this manuscript.

Physical and biogeochemical spatial scales of variability in the East Australian Current separation from shelf glider measurements

Amandine Schaeffer¹, Moninya Roughan¹, Emlyn Jones², and Dana White¹

¹Coastal and Regional Oceanography Lab, School of Mathematics and Statistics, University of New South Wales, Sydney NSW, 2052, Australia

²CSIRO Oceans and Atmosphere, Hobart, Tasmania, Australia

Correspondence to: Amandine Schaeffer (a.schaeffer@unsw.edu.au)

Abstract. In contrast to physical processes, biogeochemical processes are inherently patchy in the ocean, which affects both the observational sampling strategy and the representativeness of sparse measurements in data assimilating models. In situ observations from multiple glider deployments are analyzed to characterize spatial scales of variability in both physical and biogeochemical properties, using an empirical statistical model. We find that decorrelation ranges are strongly dependent on the balance between local dynamics and mesoscale forcing. The shortest horizontal (5-10 km) and vertical (45 m) decorrelation ranges are for chlorophyll-a fluorescence. Whereas those variables that are a function of regional ocean and atmosphere dynamics (temperature and dissolved oxygen) result in anisotropic patterns with longer ranges along (28-37 km) than across the shelf (8-19 km). Variables affected by coastal processes (salinity and colored dissolved organic matter) have an isotropic range similar to the baroclinic Rossby radius (10-15 km).

1 Introduction

At the interface between oceanic and coastal processes, continental shelf regions are characterized by complex dynamics resulting from the interaction between different water masses at smaller spatial scales than the open ocean (Yoder et al., 1987). While wind, topography or density driven processes mostly influence the mixing and advection of the physical characteristics (temperature and salinity) of the shelf water masses, locally acting ecological processes are also determinant for biogeochemistry (Ballantyne et al., 2011). In particular, the numerous mechanisms driving phytoplankton distributions have been studied for many years, and highlight the complexity of these interactions (Martin, 2003). Biogeochemical (BGC) processes operate over a wide range of scales and thus need to be considered separately when investigating the dominant length scales of variability for the shelf water's properties (Pan et al., 2014).

The continental shelf off southeastern Australia (between 29 and 34°S) is relatively narrow, between 16 and 70 km (mean of 37 km) from the coastline to the 200 m isobath. The dynamics on the shelf are influenced both by local coastal processes and the episodic intrusion of the large scale East Australian Current (EAC) and its eddies (Fig. 1, Schaeffer et al. (2013, 2014a)). The EAC is the western branch of the subtropical gyre in the South Pacific. It is a warm and dynamic poleward flowing current, encroaching on the continental shelf of southeastern Australia between 18°S (Ridgeway and Godfrey, 1994) and usually 30.7 - 32.4°S (Cetina-Heredia et al., 2014) where it bifurcates eastward, forming the Tasman Front. Further south, eddies are shed (Everett et al., 2012), leading to high variability in the velocity field and water masses on the shelf (Schaeffer et al., 2014b; Schaeffer and Roughan, 2015).

Previous studies have highlighted the high spatial heterogeneity of physical (Oke et al., 2008; Schaeffer and Roughan, 2015) and biochemical (Hassler et al., 2011) variables on this narrow shelf. De-correlation time scales were quantified from *in situ* mooring observations at 30° and 34° (Roughan et al., 2013), being of the order of hours for ~~aeross-shelf~~cross-shelf velocity to days and weeks for along-shelf flow and temperature, respectively. However, spatial scales of variability, which are essential for data assimilating models, have not been quantified.

Here we quantify for the first time the spatial scales of variability of both the physical and the BGC characteristics of the shelf water masses in the highly dynamic EAC separation zone. We use hydrographic measurements from 23 glider deployments along the coast (Section 2) to understand the variability amongst physical and BGC properties, the spatial anisotropy and the unresolved variance in the rich dataset (Section 3). Finally the results are discussed in the context of their applicability to modelling and data assimilation, where the perennial issue of relating point based measurements to model solutions is discussed (Section 4).

2 Methods

2.1 The Dataset

Ocean gliders are autonomous underwater vehicles which ~~use seawater to~~ change their buoyancy ~~, diving to dive up~~ through the water column ~~without using propulsion while recording~~. ~~Without propulsion, this vertical motion is transformed into horizontal momentum using the vehicle's wings, while its pitch controls the forward motion. During the resulting vertical sawtooth pattern through the water column,~~ a wealth of scientific observations ~~are recorded and analysed here~~. Physical and ~~biogeochemical~~BGC measurements from 23 ocean glider deployments along the southeastern coast of Australia are used in this study. The glider missions span all seasons over 6 years, between 2008 - 2014, including results from both shallow-diving Slocum (<200m) and deep-diving Seaglider

($<1000\text{m}$) vehicles. The gliders were typically deployed at 29.4°S although some were deployed
60 as far south as 33°S (Fig. 1 and Schaeffer and Roughan (2015)). Missions range from 2-3 weeks
to three months depending on the vehicle. The ~~average~~ horizontal displacement between two dives
~~is around~~ increases with the depth of the dive, with median over ground distances from 130 m (for
dives in 25 - 50 m of water) to 1100 m (in 150 - 200 m, while the fast sampling frequency leads to
fine vertical resolution (m of water). The vertical resolution of observations is $<2\text{ m}$ due to the fast
65 sampling frequency.

Scientific measurements include depth, temperature and salinity (from a Seabird-CTD), dissolved
oxygen (DO, from Aanderaa or Seabird Oxygen sensors), and optical parameters, chlorophyll-a flu-
orescence (excited / emitted wavelengths: 470 / 695 nm), colored dissolved organic matter (CDOM,
excited / emitted wavelengths: 370 / 460 nm) and backscatter coefficient at 650-700 nm (from a
70 WETLabs optical sensor).

Quality control for physical parameters (temperature and salinity) and DO are conducted follow-
ing ARGO standards (Wong et al., 2014), including a salinity spike correction due to the use of
unpumped CTDs in early deployments. For bio-optical parameters, quality control is more chal-
75 lenging due to the instrument bio-fouling and the high temporal and spatial variability of the mea-
surements. ~~Sensor drift is checked using pre- and post-deployment performance tests~~ Sensors are
calibrated approximately every 2 years. To check for sensor drift, performance tests are undertaken
using purple and black solid standards ~~and sensors are calibrated approximately every 2 years. The~~
~~same tests are conducted pre-, post-deployment and also~~ after cleaning the sensor from bio-fouling ~~to~~
80 ~~check for sensor drift.~~ These tests enable the identification and flagging of suspect measurements. A
global range test is also conducted with a valid fluorescence maximum set to 50 mg m^{-3} , similar to
ARGO standards (Claustre, 2011). A valid regional maximum for CDOM is defined, based on all
the shelf glider deployments, as the mean plus 10 times the standard deviation (~~= 8.02~~ 8.0 ppb) to
~~removed~~ remove high outliers (reaching 250 ppb).

85

2.2 Characterising spatial variability

The semivariogram approach was first introduced in geostatistics (Journel and Huijbregts, 1978)
to characterize the spatial variability of a sparsely distributed dataset. It describes the average dis-
similarity between measurements as a function of the distance separating them. This difference is
90 generally small for measurements within close proximity, increasing with distance, until it does not
depend on a spatial lag (decorrelated values) (Legaard and Thomas, 2007; Tortell et al., 2011).

For a variable anomaly $Z(x)$, the semivariogram or structure function, $\gamma(h)$, is defined as ~~half~~ the mean square difference between values at a given separation h :

$$95 \quad \gamma(h) = \frac{1}{2} \underline{\text{variance}[Z(x) - Z(x+h)]} \frac{1}{N} \sum ([Z(x) - Z(x+h)]^2) \quad (1)$$

where ~~h is the distance separating the two observations~~ the sum is over all N pairs of observations that are separated by the distance h in the x direction.

In order to take into account outliers in the distribution of the empirical anomalies Z , Cressie and Hawkins (1980) proposed a ~~robust-modified~~ estimate of the structure function which is more robust
 100 when the anomaly fields deviate from being Gaussian:

$$\gamma(h) = \frac{\frac{1}{2} \left(\frac{1}{N} \sum [Z(x) - Z(x+h)]^{1/2} \right)^4}{0.457 + \frac{0.494}{N}} \frac{\frac{1}{2} \left(\frac{1}{N} \sum [Z(x) - Z(x+h)]^{1/2} \right)^4}{0.457 + \frac{0.494}{N}} \quad (2)$$

~~where the sum is over all N pairs of measurements that are separated by the distance h~~ In this equation, the power 1/2 comes from a fourth-root of $[Z(x) - Z(x+h)]^2$ that reduces the skewness
 105 in the distribution, thereby approaching a Gaussian process. The 4th square acts to correct the scale and returns the same units as equation 1, while the denominator adjusts the bias resulting from the whole transformation. This estimate is more robust statistically in the sense that the mean can be applied to the new distribution. Compared to equation 1, the semivariogram is only slightly modified for the highest lags when using the robust equation 2, but the parameters (sill, range and nugget that
 110 are investigated in section 3) remain very similar.

The variables ~~anomaly~~ anomalies are obtained by removing large scale patterns, resulting from the average of all glider measurements over predefined bins determined by latitude and depth as in ~~Schaeffer and Roughan (2015)~~ Schaeffer and Roughan (2015); Schaeffer et al. (2016). This three-dimensional
 115 mean state is then smoothed using a spline method before being removed from each observation.

Both ~~aeross-cross~~ and along-shelf semivariograms are calculated to investigate anisotropy, where $h = \Delta x$ is the zonal distance, or $h = \Delta y$ is the meridional distance, respectively. The cross-shelf ~~structure-function-semivariance~~ is calculated following equation 2 from measurement pairs located within 0.1° (~ 10 km) of latitude. Similarly, the along-shelf structure $\gamma(h)$ is computed using ob-
 120 servations within 0.1° of longitude (~ 10 km) from each other. In both cases the distance vector is discretized with intervals of 500 m and the time lag between pairs is limited to 1 day. The semivariograms are calculated in the horizontal plane at three depths: surface (~~0-50~~ 5 m), mixed layer depth (MLD, 5 - 30 m, defined from the average profiles), or below the MLD at 50 m. Finally, glider profiles are also used to analyse vertical scales by computing $\gamma(h)$ with $h = \Delta z$ (intervals of 1 m).

125 The semivariance $\gamma(h)$ is computed from the trimmed mean (20 % outliers excluded) of measurements over all glider deployments, provided there are at least 10 (5 for CDOM across the shelf, see

[section 3.4](#)) different missions and more than 30 pairs for each spatial lag, to avoid seasonal bias or insignificant values. We then fit a [mathematical](#) spherical model (Doney et al., 2003) to the empirical semivariogram in order to extract the physical characteristics of the function, following:

$$\begin{cases} \sigma_0^2 + (\sigma^2 - \sigma_0^2) \left(\frac{3}{2} \frac{h}{r} - \frac{1}{2} \left(\frac{h}{r} \right)^3 \right) & 0 < h \leq r \\ \sigma^2 & h > r \end{cases} \quad (3)$$

where h is the distance between measurements, σ^2 is the sill, σ_0^2 is the nugget and r the range. (These variables are described physically in the example below.) Exponential and Gaussian models (Biswas and Si, 2013) were also tested but were less adequate in terms of sum of squared error (sse) and adjusted R-square statistics for the fit [of the empirical semivariogram](#).

3 Results

3.1 Satellite derived SST semivariogram

By way of both example and validation we calculate the [aeross-shelf-cross-shelf](#) semivariogram obtained from daily satellite remote sensed [SST-sea surface temperature \(SST\)](#) anomalies (Fig. 2). The spherical model (Eq. 3) is fitted to the empirical semivariance values calculated for [aeross-shelf-cross-shelf](#) lags over daily maps of SST in 2014. Only days with spatial coverage greater than 30 % of the domain are considered. The physical characteristics extracted from the model are indicated in Fig 2. The sill σ^2 reflects the constant background variability of the variable. It is reached at a specific distance, here $r = 24$ km, which is referred to as the [\(decorrelation\)](#) range or the dominant length scale. For lags greater than this range, the two observations are considered randomly correlated spatially. The nugget, σ_0^2 , is the semivariance obtained from the model at the origin. If different from 0, it implies variability at shorter spatial scales than those resolved by the observations. This variability is either a) real but unresolved, or b) resulting from measurement errors. The semivariogram for SST (Fig. 2) shows very little nugget effect, showing the accuracy of the measurements and an adequate spatial resolution.

As expected, the semivariance of the SST anomaly (the annual mean was subtracted) differs with seasonality, as shown by the monthly empirical semivariograms (Fig. 2). Austral Summer and Autumn months are characterized by a sharper increase in the SST variance with greater variability in sills, due to more pronounced spatial temperature gradients. However, the [semivariogram](#) range is similar, with dominant [aeross-shelf-cross-shelf](#) scales between 18 km and 32 km (not shown). The [structure function reached-semivariogram reaches](#) a plateau for all months with the exception of January, suggesting a trend of longer scales (Yoder et al., 1987) and a limitation of the method.

160 3.2 Sill: *In situ* spatial variance

Semivariance values from glider measurements are analysed based on the values of the sill in each of the semivariograms shown in Fig. 3. Temperature, dissolved oxygen (DO), and to a lesser extent colored dissolved organic matter (CDOM) and salinity, are characterised by a greater variance in the vertical than in the horizontal (see the different y-axis). In contrast, chlorophyll-a fluorescence
165 shows comparable variability in all directions.

Focusing on horizontal sills (Fig. 3 middle and left), the highest variance for salinity and CDOM occurs at the surface in agreement with the influence of riverine input. The cross-shelf sill for DO is greater at 50 m than at the surface, suggesting more spatial variability due to bio-physical processes (remineralsation, respiration or bottom water uplift) than resulting from gas exchange with the at-
170 mosphere. Chlorophyll-a fluorescence shows little variance at 50 m depth due to light limitation preventing biological activity. The highest horizontal sill for temperature appears below the MLD along the shelf, in agreement with the large latitudinal gradients in bottom temperature evidenced by Schaeffer and Roughan (2015). The surface temperature sill is smaller when measured by the gliders (Fig. 3) than by satellite (Fig. 2), possibly due to different measurement depth (*in situ* 0-5 m
175 versus skin SST), or seasonality, as glider deployments are more numerous in winter. Nevertheless, the across-shelfcross-shelf dominant length scales are in good agreement in the two datasets, with ranges of 25 and 19 km, respectively.

3.3 Range: *In situ* scales of variability

180 Across-shelfCross-shelf, along-shelf and vertical ranges from the semivariograms are presented in Fig. 3 and summarized in Table 1. Spatial scales highlight different directional patterns between the parameters. Horizontal scales for salinity and CDOM are 9-15 km, 5-10 km for chlorophyll-a, similar across and along the shelf. Mean temperature rangesscales across the shelf are 18-19 km at the surface and in the MLD, only 14 km at 50 m. Scales found along the shelf are greater, be-
185 ing 28-29 km and 37 km, respectively. This directional anisotropy for temperature is in agreement with the geometry of the shelf and the influence of the EAC at the shelf break (Fig. 1). Schaeffer and Roughan (2015) and Oke et al. (2008) both evidenced greater temperature gradients across than along the shelf, based on satellite, model and glider datasets. This directional anisotropy is also evident in density (not shown), which has been shown to be mostly temperature driven (Schaeffer
190 et al., 2014b), and even more intensified for DO. While DO is characterized by dominant across shelfcross-shelf scales similar to salinity and CDOM (8 - 15 km), the along-shelf spatial variability seems to be linked to the shallow EAC watermass, resulting in rangesdecorrelation scales of 27 - 35 km (surface and MLD) similar to temperature.

Chlorophyll-a fluorescence has the smallest characteristic rangelength scales both across and along

195 the shelf, but also in the vertical. Measurements of fluorescence are decorrelated for depth lags greater than 46 m, in agreement with shallow (near surface) chlorophyll blooms. Vertical length scales for DO and CDOM (57 - 58 m), are less than those for temperature and salinity (62 m and 66 m, respectively).

The second peak in semivariance (at 80 - 100 m for temperature, salinity and DO, Fig. 3, right) 200 indicates an anti-correlation for these lags (Legaard and Thomas, 2007). Negative correlation coefficients reaching -0.6 were previously observed from moored autumnal temperature observations in 100 m water depth at ~~-30~~30°S (Roughan et al., 2013) and attributed to simultaneous heating source in the surface layers and cooling at depth due to EAC encroachments and slope water uplift. Our results suggest that these current-driven uplifts are associated with a fresher and lower DO signature. 205

3.4 Nugget: *In situ* unresolved variance

The fraction of resolved and unresolved variance is estimated from the semivariogram parameters, the sill and nugget, respectively. A nugget occurs when the difference between the two closest measurements is greater than 0, and can be seen at the origin of the semivariogram.

210 Overall, the high density glider observations capture most of the spatial ocean variability. The advantage of this sampling strategy is that nearly all the vertical variance is resolved for most of the parameters (ratio $\sigma_0^2/\sigma^2 \sim 0 - 3\%$, Table 1) due to the high sampling frequency of the gliders compared to their vertical displacement velocity. The only exception is for CDOM with the nugget being 24% of the total variance (Fig. 3 and Table 1).

215 Horizontal variability is well resolved for temperature and salinity with ratios $\sigma_0^2/\sigma^2 \leq 10\%$ across the shelf, mostly $\leq 14\%$ along the shelf. Nuggets for BGC parameters are higher, especially for chlorophyll-a fluorescence and CDOM measurements. While high nuggets for fluorescence can be attributed to horizontal sub-scale unresolved biological activity, CDOM datasets might suffer from measurement errors and quality control issues, as suggested by the high nugget effect in the vertical ~~and~~, the large outliers and the larger amount of cross-shelf lags necessary for the successful fit of a mathematical model (see section 2). 220

4 Discussion

This study combines in situ measurements from multiple glider deployments between 2008 - 2014 225 on the southeastern Australian continental shelf, to provide insight into the surface and sub-surface structure of the water-mass dynamics, including the influence of the EAC, upwelling and freshwater inputs. Analysis of ~~length-scale~~ length scale dependent variability demonstrates that much of the spatial variance in physical and BGC parameters typically occurs at scales ranging 5 km for

chlorophyll-a fluorescence to ~35 km for along-shelf temperature.

230 In this study the length scales were averaged from data obtained over 2 degrees of latitude, however we expect more regional variability resulting from the different latitudinal regimes evidenced by Schaeffer and Roughan (2015), driven by the meso-scale circulation. In addition, we expect that spatial scales may vary seasonally, particularly in the biological parameters. This will be tested when we have sufficient data in each season.

235 ~~Uncertainties can~~

~~As for all statistics, limitations~~ arise from the ~~semivariogram method, amount of data used~~ (especially along the shelf where the data density is smaller. ~~However~~) ~~and contamination of the dataset (for instance CDOM). In geostatistics, uneven spatial distribution of the observations over the analyzed area can be a limitation as well but remains difficult to quantify. The major advantage of the semivariogram~~
240 ~~method used is that it can be applied to sparse dataset like glider observations, as opposed to spatial autocorrelations for instance. It allows objective comparison of interesting parameters (range, sill, nugget) for different variables, directions and depths. In this study,~~ the results compare well when using different statistical fits, and are consistent with expected outcomes based on ~~previous knowledge of local dynamics and~~ related studies in other regions.

245 4.1 Related studies

From a global analysis of satellite derived surface data, Doney et al. (2003) found comparable small-scale variability for biology and physics. However, they were not able to characterize scales <15 km based on the satellite products used. Here we find that BGC distribution occurs predominantly at submesoscales (5 - 15 km for chlorophyll-a, CDOM), while scales for temperature are larger (18 -
250 37 km). These short scales of variability for BGC are in agreement with the effect of nutrient cycling, reproductive rate and community interaction (e.g. grazing pressure from zooplankton) that can lead to patches of 5-10 km (Ballantyne et al., 2011; Denman et al., 1977; Goebel et al., 2014).

According to Mahadevan and Campbell (2002), the fine scale patchy distribution of phytoplankton is linked to the short characteristic time in response to disturbance in their concentration, as opposed
255 to the longer time for temperature to adjust to external forcing. We find temperature horizontal scales (18 - 37 km) that are of the same order of magnitude as over the Malvinas current region, derived from SST (20 - 47 km, Tandeo et al. (2014)) or over the Middle Atlantic Bight from *in situ* glider observations (10 - 35 km, Todd et al. (2013)). The anisotropic shape of the temperature variance is consistent with a highly dynamic circulation (Tandeo et al., 2014), here driven by the EAC, characterized by a greater signature in temperature than in salinity.
260

Spatial variability in salinity is predominantly isotropic and similar to CDOM with ~~ranges decorrelation~~ ~~length scales~~ of 9 - 15 km, corresponding to the first Rossby baroclinic radius of deformation (12 - 15 km based on local moored observation, Schaeffer et al. (2014b)), and high surface variance,

suggesting a predominant influence of coastal processes and river input.

265

4.2 Drivers of variability in a modelling perspective

Assuming that there is no first order feedback from the biology to the physics, we can think of the physics variables $\mathbf{X} = T, S$ (temperature and salinity) being a function of internal dynamics (I , e.g. mixing), atmospheric forcing (A), coastal buoyancy forcing arising from river discharge (R), friction due to shallow bathymetry (F) and open ocean forcing (e.g. tidal, geostrophy) and water masses (O). Therefore the state of the model at some spatial location " s " at time t is given by:

$$\mathbf{X}(s, t) = f(I, A, R, F, O) \quad (4)$$

where $f(I, A, R, F, O)$ for the physical variables can be solved numerically in various hydrodynamic models.

275 For the state variable of temperature, we assume that there is little effect from river input in this region (e.g. water coming in is about the same temperature as the surface layer), while the effect from coastal processes is large for salinity. Therefore [eq. Eq. 4](#) simplifies to:

$$T(s, t) = f(I, A, F, O) \quad (5)$$

$$280 \quad S(s, t) = f(I, A, R, F, O) \quad (6)$$

Given that both T and S are subjected to the same advection and diffusion equations, but differ only in the source/sink and boundary terms of $f(A)$, $f(R)$ and $f(O)$, ~~this is the major driver~~ those are the major drivers for the difference in the along shelf sills and differences in the nugget. Salinity varies over shorter length scales due to river input and the markedly different freshwater inputs from various catchment sizes along the coast. Whereas temperature is largely controlled by the regional scale EAC forcing and the relatively smooth atmospheric forcing applied which varies over spatial scales of 50 km or more.

A similar approach can be applied to the BGC variables, but $f(I)$ is more complicated as it includes the turnover of biomass/nutrients between different plankton functional types or nutrient pools. But ultimately, one would expect $f(I)$ to introduce variability at scales equal to or less than those seen in salinity. This hypothesis is supported by the ranges reported in the chlorophyll-a fluorescence and CDOM variables, which are biologically derived. However, as CDOM can also be introduced into the coastal ocean via river plumes and has a similar sill to salinity, we suggest that the CDOM measured by the glider is largely due to river discharge. The DO distribution in the surface layer is largely a function of air-sea exchange and will have similar variability to temperature due to the forcing mechanism. However, below the mixed layer, DO is function of the remineralisation rate and

295

also vertical mixing/exchange with surface water, explaining the shorter decorrelation range in DO found below the mixed layer.

300 4.3 Observing system design

The length scales calculated here can be used to guide the design of ocean observing systems. ~~To~~ , in particular to answer questions related to the observation density needed to resolve along and ~~aeross-shore~~ cross-shore variability in both the physical and biological parameters. The temperature anisotropy in our results, consistent with findings of Oke and Sakov (2012) and Jones et al. (2015),
305 shows that the required observation density will vary along and across the shelf. Thus high resolution ~~aeross-shelf~~ cross-shelf mooring or glider lines every Y km are more useful than simply a glider endurance line or equally spaced moorings. The distance Y can be initially derived from satellite observations, or determined after a number of glider missions. In contrast, the understanding of BGC variability, characterized by short isotropic length scales, will require high spatial resolution
310 observations (e.g. gliders) to determine the representativeness of the measurements.

4.4 Data assimilation

There are a variety of data assimilation systems based upon two broad approaches, ensemble methods (e.g. Oke et al. (2008), Jones et al. (2012)) and variational methods, that minimize a cost function (e.g. Moore (2011)). Regardless of the approach used, assumptions are made about the spatial footprint of an observation, for which a key parameter is the decorrelation length scale. Within the ensemble (e.g. Oke et al. (2008)) and hybrid (Pan et al., 2011) data assimilation approaches, covariance localization (Sakov and Bertino, 2011) is used to increase the rank of the background error covariance matrix. The anisotropic (along-shelf and cross-shelf) ranges presented in this study and method used to derive them, allow for the direct calibration of the decorrelation scales enforced within most data assimilation systems that are currently in use. Additionally, estimates of how these decorrelation scales vary in time is also available (e.g. Figure 2), suggesting that an optimally tuned data assimilation system should allow for temporal variation in the localization or provide an assessment of the temporal variability of the ensemble from an an Ensemble Kalman Filter (EnKF) system.
315
320
325

The results from this study also allow us to partly answer the question of how to relate a point based observation with the output from a numerical model, which assumes the average concentration of a variable within a model cell X_{mod} . If we take a Bayesian view stating that we observe some
330 true state variable with error (e.g. Parslow et al. (2013)), this can be written as:

$$X_{obs} = X_{true} + \epsilon_m + \epsilon_v \quad (7)$$

where X_{obs} is the observed variable, X_{true} is the true unknown value of the variable, ϵ_m is the instrument error and ϵ_v is the sampling error due to unresolvable small scale variability. The observation is then related to the modelled variable by:

335
$$X_{mod} = X_{obs} + \epsilon_r \tag{8}$$

where ϵ_r is typically referred to as the representation error (Oke and Sakov, 2008) associated with difference in kind (e.g. measuring fluorescence, but modelling biomass), or averaging across a model grid cell that contains a point measurement.

Assuming ϵ_m is known from calibration studies, results of studies like that presented here allow us
340 to explore the characteristics of ϵ_v and ϵ_r . For a particular variable, we can assume that the nugget is approximately equal to ϵ_v and given a-priori information about a model grid, the spherical model applied to the ~~semi-variogram can then~~ semivariogram can then also be used to provide an empirical estimate ~~not only for ϵ_r , but if observations are ingested into a data assimilation system, the estimates of the anisotropic range can be used to then tune the localization function (e.g. Oke et al. (2007))~~
345 ~~applied to each observation~~.

To this end, the results of this study allow us to characterise the length scales of the physical and BGC properties on the shelf and relate variability to the dynamical drivers, but additionally, the methodology developed here can be directly used to improve observing system design, and to tune
350 key data assimilation parameters that are presently poorly understood.

Acknowledgements. IMOS is an initiative of the Australian Government being conducted as part of the National Collaborative Research Infrastructure Strategy. Assistance with logistical and technical support for this project has been provided by ANFOG - Australian Facility for Ocean Gliders and the NSW-IMOS glider team. All datasets are freely available at <http://www.imos.org.au>.

355 **References**

- Ballantyne, F., O. M. Schofield, and S. Levin, 2011: The emergence of regularity and variability in marine ecosystems: the combined role of physics, chemistry and biology. *Scientia Marina*, **75** (4).
- Biswas, A. and B. C. Si, 2013: *Model Averaging for Semivariogram Model Parameters, Advances in Agrophysical Research*, chap. 4, 81–96. doi:10.5772/52339.
- 360 Cetina-Heredia, P., M. Roughan, E. van Sebille, and M. A. Coleman, 2014: Long-term trends in the east australian current separation latitude and eddy driven transport. *Journal of Geophysical Research: Oceans*, **119**, 4351–4366, doi:10.1002/2014JC010071.
- Claustre, H., 2011: Bio-optical sensors on argo floats. reports of the international ocean-colour coordinating group, no. 11, ioccg. Tech. rep., IOCCG, Dartmouth, Canada.
- 365 Cressie, N. and D. Hawkins, 1980: Robust Estimation Of The Variogram. *Journal Of The International Association For Mathematical Geology*, **12** (2), 115–125, doi:10.1007/BF01035243.
- Denman, K., A. Okubo, and T. Platt, 1977: The chlorophyll fluctuation spectrum in the sea. *Limnology and Oceanography*, **22** (6), 1033–1038, doi:10.4319/lo.1977.22.6.1033.
- Doney, S. C., D. M. Glover, S. J. McCue, and M. Fuentes, 2003: Mesoscale variability of sea-viewing wide field-of-view sensor (seawifs) satellite ocean color: Global patterns and spatial scales. *Journal of Geophysical Research: Oceans*, **108** (C2), 3024, doi:10.1029/2001JC000843.
- 370 Everett, J. D., M. E. Baird, P. R. Oke, and I. M. Suthers, 2012: An avenue of eddies: Quantifying the biophysical properties of mesoscale eddies in the Tasman Sea. *Geophys. Res. Lett.*, **39**, L16 608, doi:10.1029/2012GL053091.
- 375 Goebel, N. L., S. Frolov, and C. A. Edwards, 2014: Complementary use of wave glider and satellite measurements: Description of spatial decorrelation scales in chl-a fluorescence across the pacific basin. *Methods in Oceanography*, **10** (0), 90 – 103, doi:http://dx.doi.org/10.1016/j.mio.2014.07.001.
- Hassler, C., J. Djajadikarta, M. Doblin, J. Everett, and P. Thompson, 2011: Characterisation of water masses and phytoplankton nutrient limitation in the east australian current separation zone during spring 2008. *Deep Sea Research Part II: Topical Studies in Oceanography*, **58** (5), 664 – 677, doi:10.1016/j.dsr2.2010.06.008.
- 380 [Oke, P. R., F. Rizwi and L. M. Murray, 2008: Assimilation of glider and mooring data into a coastal ocean model. *Ocean Modelling*, **47**, 1–13. doi:10.1016/j.ocemod.2011.12.009.](#)
- Jones, E. M., M. A. Doblin, R. Matear, and E. King, 2015: Assessing and evaluating the ocean-colour footprint of a regional observing system. *Journal of Marine Systems*, **143** (0), 49 – 61, doi:http://dx.doi.org/10.1016/j.jmarsys.2014.10.012.
- 385 Journal, A. G. and C. J. Huijbregts, 1978: *Mining geostatistics*. Academic Press London ; New York, x, 600
- Legaard, K. R. and A. C. Thomas, 2007: Spatial patterns of intraseasonal variability of chlorophyll and sea surface temperature in the california current. *Journal of Geophysical Research: Oceans*, **112** (C9), 006, doi:10.1029/2007JC004097.
- 390 Mahadevan, A. and J. W. Campbell, 2002: Biogeochemical patchiness at the sea surface. *Geophysical Research Letters*, **29** (19), 32–1–32–4, doi:10.1029/2001GL014116.
- Martin, A., 2003: Phytoplankton patchiness: the role of lateral stirring and mixing. *Progress in Oceanography*, **57** (2), 125 – 174, doi:http://dx.doi.org/10.1016/S0079-6611(03)00085-5.

- 395 [A. M. Moore, H. G. Arango, G. Broquet, C. Edwards, M. Veneziani, B. Powell, D. Foley, J. D. Doyle, D. Costa, P. Robinson, 2011: The Regional Ocean Modeling System \(ROMS\) 4-dimensional variational data assimilation systems: Part II - Performance and application to the California Current System. *Progress in Oceanography*, **91**, 50 – 73, doi:10.1016/j.pocean.2011.05.003.](#)
- Oke, P. and P. Sakov, 2012: Assessing the footprint of a regional ocean observing system. *Journal of Marine Systems*, **105–108** (0), 30 – 51, doi:10.1016/j.jmarsys.2012.05.009.
- 400 Oke, P. R., G. B. Brassington, D. A. Griffin, and A. Schiller, 2008: The blueink ocean data assimilation system (bodas). *Ocean Modelling*, **21** (1-2), 46 – 70, doi:10.1016/j.ocemod.2007.11.002.
- Oke, P. R. and P. Sakov, 2008: Representation Error of Oceanic Observations for Data Assimilation. *Journal of Atmospheric and Oceanic Technology*, **25**, 1004, doi:10.1175/2007JTECHO558.1.
- Oke, P. R., P. Sakov, and S. P. Corney, 2007: Impacts of localisation in the enkf and enoi: experiments with a small model. *Ocean Dynamics*, **57** (1), 32–45.
- 405 [Pan, C., M. Yaremchuk, D. Nechaev, and H. Ngodock, 2011: Variational assimilation of glider data in Monterey Bay. *Journal of Marine Research*, **69** \(2-3\), 331 – 346, doi:10.1357/002224011798765259.](#)
- Pan, C., L. Zheng, R. H. Weisberg, Y. Liu, and C. E. Lembke, 2014: Comparisons of different ensemble schemes for glider data assimilation on west florida shelf. *Ocean Modelling*, **81**, 13 – 24, doi:10.1016/j.ocemod.2014.06.005.
- 410 Parslow, J., N. Cressie, E. P. Campbell, E. Jones, and L. Murray, 2013: Bayesian learning and predictability in a stochastic nonlinear dynamical model. *Ecological applications*, **23** (4), 679–698.
- Ridgeway, K. and J. Godfrey, 1994: Mass and heat budgets in the east australian current: a direct approach. *Journal of Geophysical Research*, **99**, 3231–3248.
- 415 Roughan, M., A. Schaeffer, and S. Kioroglou, 2013: Assessing the design of the nsw-imos moored observation array from 2008-2013: Recommendations for the future. *Oceans - San Diego, 2013*, 1–7.
- ~~Schaeffer, A. and M. Roughan, 2015: Influence of a western boundary current on shelf dynamics and upwelling from repeat glider deployments.~~
- [Sakov, P. and L. Bertino, 2011: Relation between two common localisation methods for the EnKF. *Geophysical Research Letters*, **42** \(1\), 121–128, *Computational Geosciences*, **15** 2, 225–237.](#) doi:10.1007/s10596-010-9202-6
- 420 ~~Schaeffer, A., M. Roughan, and B. Morris, 2013: Cross-shelf dynamics in a western boundary current. implications for upwelling. *Journal of Physical Oceanography*, **43**, 1042 – 1059, doi:10.1175/JPO-D-12-0177.1.~~
- Schaeffer, A., M. Roughan, and B. Morris, 2014a: Corrigendum cross-shelf dynamics in a western boundary current. implications for upwelling. *Journal of Physical Oceanography*, **44**, 2812–2813, doi:http://dx.doi.org/10.1175/JPO-D-14-0091.1.
- 425 Schaeffer, A., M. Roughan, and J. E. Wood, 2014b: Observed bottom boundary layer transport and uplift on the continental shelf adjacent to a western boundary current. *Journal of Geophysical Research: Oceans*, **119**, 4922 – 4939, doi:10.1002/2013JC009735.
- 430 [Schaeffer, A., and M. Roughan, 2015: Influence of a western boundary current on shelf dynamics and upwelling from repeat glider deployments. *Geophysical Research Letters*, **42**, 121 – 128, doi:10.1002/2014GL062260.](#)

Schaeffer, A., M. Roughan, T. Austin, B. Hollings, E. King, A. Mantovanelli, S. Milburn, B. Pasquer, C. Pattiaratchi, R. Robertson, I. Suthers, D. White : Mean hydrography on the continental shelf from 25 repeat glider deployments along Southeastern Australia. *Scientific Data*, **in review**.

435

Tandeo, P., E. Autret, B. Chapron, R. Fablet, and R. Garello, 2014: {SST} spatial anisotropic covariances from metop-avhrr data. *Remote Sensing of Environment*, **141** (0), 144 – 148, doi:<http://dx.doi.org/10.1016/j.rse.2013.10.024>.

440

Todd, R. E., G. G. Gawarkiewicz, and W. B. Owens, 2013: Horizontal scales of variability over the middle atlantic bight shelf break and continental rise from finescale observations. *J. Phys. Oceanogr.*, **43**, 222–230, doi:<http://dx.doi.org/10.1175/JPO-D-12-099.1>.

Tortell, P., C. Gueguen, M. Long, C. Payne, P. Lee, and G. DiTullio, 2011: Spatial variability and temporal dynamics of surface water pCO₂, O₂/Ar and dimethylsulfide in the Ross Sea, Antarctica. *Deep Sea Research Part I: Oceanographic Research Papers*, **58** (3), 241 – 259, doi:<http://dx.doi.org/10.1016/j.dsr.2010.12.006>.

445

Wong, A., R. Keeley, and T. Carval, 2014: Argo quality control manual. Tech. rep., Argo Data Management Team. doi:<http://dx.doi.org/10.13155/33951>.

Yoder, J. A., C. R. McClain, J. O. Blanton, and L.-Y. Oeymay, 1987: Spatial scales in czcs-chlorophyll imagery of the southeastern u.s. continental shelf. *Limnology and Oceanography*, **32** (4), 929–941, doi:[10.4319/lo.1987.32.4.0929](http://dx.doi.org/10.4319/lo.1987.32.4.0929).

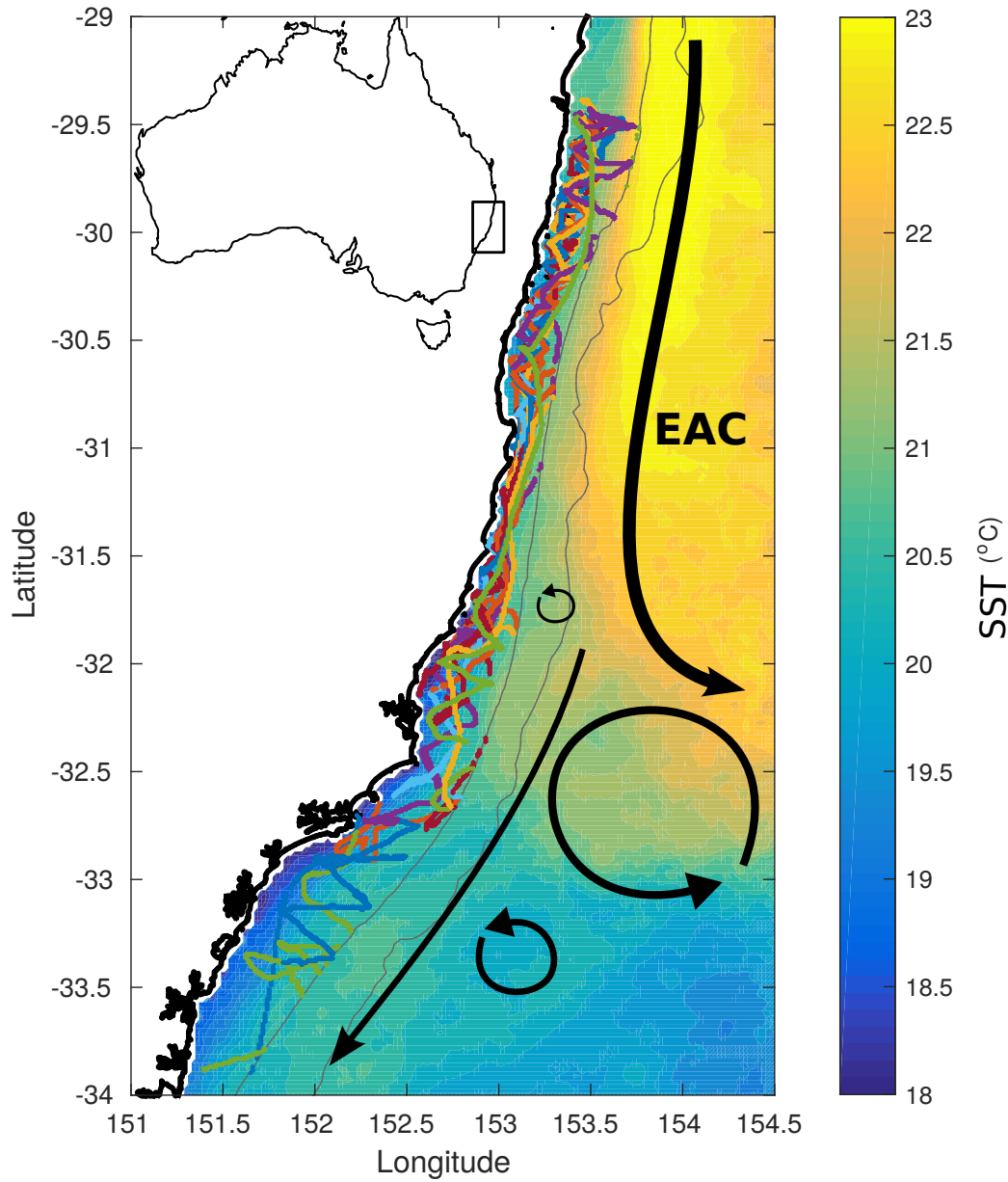


Figure 1. Monthly mean Sea Surface Temperature (GHRSSST-AVHRR L3S product) over southeastern Australia for March-October 2014. The coastline, 200 and 2000 m isobaths are shown. Glider tracks over the shelf (depth <200 m) are indicated by colored lines. A schematic of the typical circulation is shown with the poleward flowing East Australian Current (EAC) bifurcating to the East around 32°S, its weaker extension, anticyclonic and cyclonic eddies.

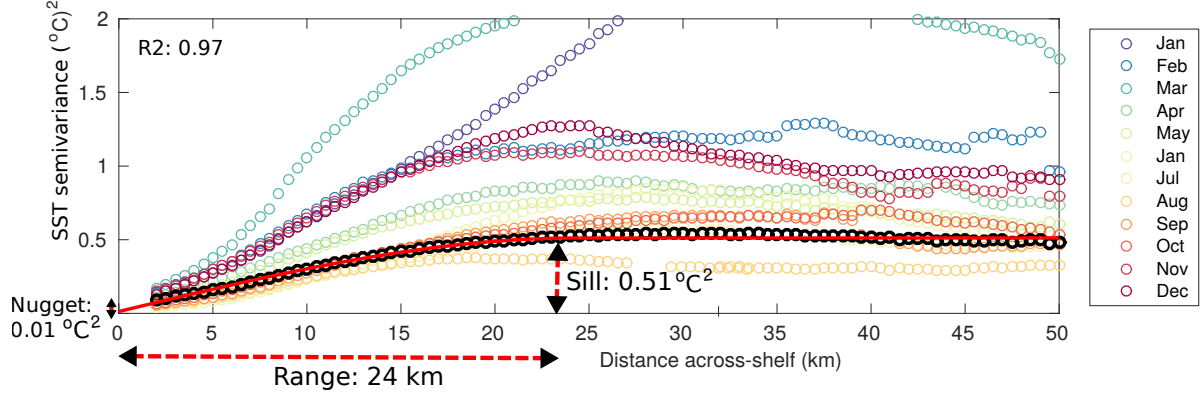


Figure 2. Across-shelf Cross-shelf empirical semivariogram estimated from daily SST over the southeastern Australian shelf (depth <200 m, 29 - 34°S, GHRSSST-AVHRR L3S product) for 2014 (black bold dots) and for each month in 2014 (colored dots). The spherical model (R-square red line, R-squared of 0.97 for the fit) and resulting parameters (range, sill, nugget) are shown in red for 2014 semivariance.

		Temperature	Salinity	Fluorescence	DO	CDOM	
Cross-shelf	Surface	range	19 km	13 km	5 km	10 km	10 km*
		ratio σ_0^2/σ^2	6 %	6 %	17%	27 %	19%
		R-squared fit	0.96	0.94	0.89	0.85	0.49
	MLD	range	18 km	10 km	8 km*	8 km	13 km
		ratio σ_0^2/σ^2	4 %	0%	13%	18%	2%
		R-squared fit	0.92	0.83	0.58	0.89	0.96
	50m	range	15 km		5 km	15 km	11 km
		ratio σ_0^2/σ^2	10%		15%	4%	17%
		R-squared fit	0.97		0.73	0.98	0.88
Along-shelf	Surface	range	30 km	15 km*	8 km	35 km	11 km*
		ratio σ_0^2/σ^2	14%	14 %	20%	2%	21%
		R-squared fit	0.93	0.52	0.83	<u>0.9</u> <u>0.90</u>	0.56
	MLD	range	28 km	10 km	10 km*	28 km	9 km*
		ratio σ_0^2/σ^2	8%	23%	21%	18 %	10%
		R-squared fit	0.99	0.93	0.53	0.96	0.27
	50m	range	37 km		5 km	4 km*	
		ratio σ_0^2/σ^2	1%		8%	5%	
		R-squared fit	0.97		0.87	0.33	
Vertical	range	62 m	66 m	46 m	58 m	57 m	
	ratio σ_0^2/σ^2	0%	3 %	1%	0%	24%	
	R-squared fit	0.97	0.98	0.99	0.98	0.99	

Table 1. Spatial scales of variability for spherical fit to robust structure functions semivariograms for different parameters and depths across, along the shelf and along the vertical. The range, percentage ratio of the nugget to the sill (σ_0^2/σ^2) and R-squared for the model fit to experimental values are also-indicated (ranges with * correspond to R-squared <0.7). Blanks indicate unsuccessful fit to the spherical model.

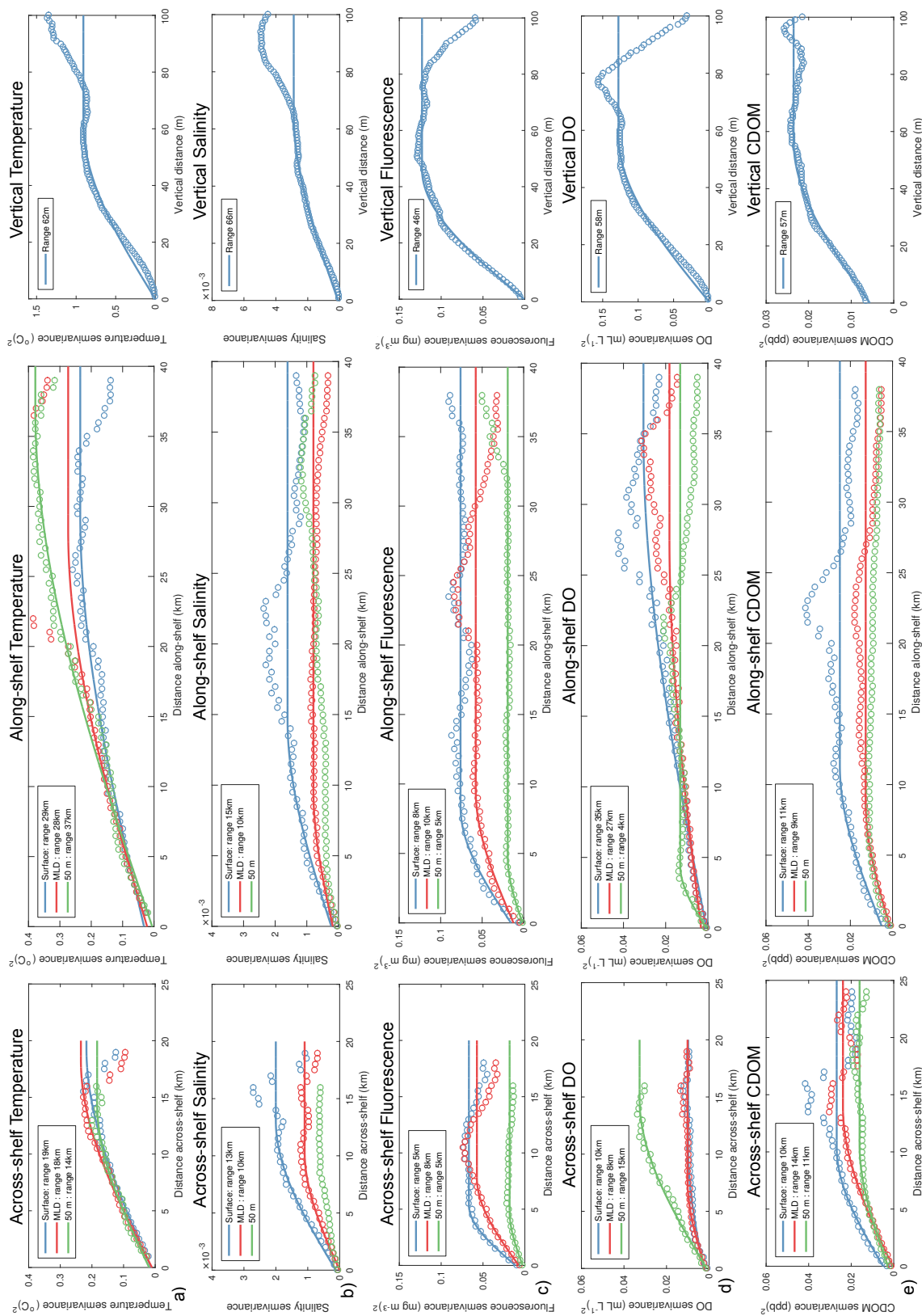


Figure 3. Across-shelf Cross-shelf (left), along-shelf (middle) and vertical (right) empirical semivariograms estimated from glider measurements of a) temperature, b) salinity, c) chlorophyll-a fluorescence, d) DO and e) CDOM. Spherical models are shown by the solid lines and the resulting spatial ranges are indicated in the insert for successful fits. Blue, red, green symbols for horizontal semivariogram semivariograms correspond to surface, MLD (0-30 m) and 50 m measurements, respectively.